



## Radiolytic degradation of reactive textile dyes by ionizing high energy ( $\gamma$ - Co<sup>60</sup>) radiation: artificial neural network modelling

V.C. Padmanaban<sup>a</sup>, N. Selvaraju<sup>b</sup>, V.N. Vasudevan<sup>c</sup>, Anant Achary<sup>a,\*</sup>

<sup>a</sup>Center for Research, Department of Biotechnology, Kamaraj College of Engineering & Technology, S.P.G.C.Nagar, K.Vellakulam - 625 701, Madurai, Tamil Nadu, India, email: vcpadmanaban88@gmail.com (V.C. Padmanaban), Tel. +91 9486823312, email: achyanant@yahoo.com (A. Achary)

<sup>b</sup>Department of Biosciences and Bioengineering, Indian Institute of Technology Guwahati, Guwahati-781039, Assam, India, email: selva@iitg.ernet.in (N. Selvaraju)

<sup>c</sup>Meat Technology Unit, Kerala Veterinary and Animal Science University, Thrissur, Kerala - 680651, India, email: vasudevan@kvasu.ac.in (V.N. Vasudevan)

Received 13 March 2018; Accepted 25 August 2018

### ABSTRACT

In this study, three artificial neural network (ANN) models were developed for the prediction and simulation of the degradation of textile dyes (Reactive Orange 16 - Monoazo; Reactive Red 120 - Diazo; Direct Red 80 - Poly azo) by high energy gamma radiation. Concentration of H<sub>2</sub>O<sub>2</sub> (0–2.0 mM), dose of gamma ray (1–6 kGy), pH (3.0–11.0), concentration of dye (100–500 mg/L) were given as inputs and the output was percentage of degradation. A three-layer feed-forward network was trained using 750 sets of input–output response per dye using Levenberg–Marquardt back propagation algorithm with ten neurons in the hidden layer. The efficiency of the trained network was validated by using sets of input operated at pH 6.0 & 12.0. The results predicted were very close to the experimental results with R<sup>2</sup>: 0.9967 for Reactive Orange 16; 0.9960 for Reactive Red 120; 0.9977 for Direct Red 80. The sensitivity analysis showed that Concentration of H<sub>2</sub>O<sub>2</sub> & Dose of gamma ray have strong effect whereas pH and concentration of dye have little effect on the degradation process. The results showed that the statistical modelling by ANN could effectively predict the behavior of radiolytic degradation of reactive dyes.

*Keywords:* Reactive dyes; Artificial neural network; Degradation; Hydrogen peroxide; Free radicals

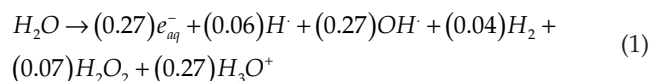
### 1. Introduction

Release of highly reactive dyes from textile industries into ground water and river water streams is one of the major environmental issue in India and China. Textile dyes have been considered in the context of recalcitrant xenobiotic compounds, as these toxic dyes are highly stable, the discarded dye remains for long-term in the environment and thus accumulates [1]. Among industrially used dyes, reactive azo and reactive anthraquinone group of dyes are largest (around 80% of dyes) and most important groups of dyes [2]. Since these reactive dyes are having fused aromatic

structure, they are highly stable and resistance towards light or oxidizing agents, physico-chemical degradation [3]. From the extensive literature survey, it was observed that the classical physical, chemical and biological treatment methods existing now is not efficient in developing a zero discharge technology (ZDT). In addressing this issue, recent technology of employing advanced oxidation processes (AOPs) for the treatment of industrial effluent is becoming prevalent. The rate of formation of hydroxyl radicals ( $\cdot$ OH) with an oxidation potential of 2.80 V determines the efficiency of the AOP in complete mineralization of highly toxic organic compounds. The application of radiation based technology for the waste water treatment is highly preferred than other AOPs because of its environment friendly nature and the

\*Corresponding author.

adaptability to intensify or to augment the generation of highly reactive oxidising species [4] (Eq. 1).



The number of micro moles of species formed per one joule of absorbed energy is given as the G value (in brackets) [5]. The concentration of hydroxyl radicals ( $\cdot OH$ ) is increased by the external addition of hydrogen peroxide to the system [6]. The hydrogen peroxide reacts with  $e_{aq}^-$  and  $H\cdot$  generated during radiolysis of water which intensifies the process [7]. The radiolysis of textile waste water is quite complex, since the mechanism of process is influenced by various process parameters, the quantification of hydroxyl radicals generated and its related kinetics, the complexity in solving the equations that involve the radiant energy balance and the spatial distribution of absorbed radiation. The modelling of these processes involves many problems which cannot be solved by simple linear multivariate correlation [8]. Artificial Neural networks (ANN) are now used in various disciplines of science and technology because of their simplicity towards simulation, prediction and modelling [9]. ANN focuses solely on solving real problems on four different aspects: (a) fault detection, (b) prediction of polymer quality, (c) data rectification (d) modeling and control. The applications of ANN are in various chemical industries like petrochemicals, oil and gas industry, biotechnology, cellular industry, environment, health and safety, fuel and energy, mineral industry, nano technology, pharmaceutical industry, and polymer industry[10]. Though, few studies were reported on ANN based prediction and modelling on various AOPs [11,12], the application of statistical prediction (ANN) on the degradation of reactive dyes by radiolysis was reported less. In this study, ANN was used to predict and simulate the degradation of reactive dyes (Reactive Orange 16 - Mono azo; Reactive Red 120 - Di azo; Direct Red 80 - Poly azo) in aqueous solution by high energy gamma radiation. A three-layer feed-forward network was trained using Levenberg–Marquardt back propagation algorithm with ten neurons in the hidden layer. The ANN modelling outputs were validated by comparing with the experimental data.

## 2. Materials and methods

### 2.1. Materials

Reactive Orange 16 (RO 16), Reactive Red 120 (RR 120) and Direct Red 80 (DR 80) were chosen as the model dyes from monoazo, diazo and polyazo class respectively. These model dyes were purchased from Sigma–Aldrich, India. The structure and characteristics of these dyes are given in Table 1. Aqueous dye solutions of different concentrations (100, 200, 300, 400, 500 mg/L) were prepared using deionized water. The pH of the irradiated and non-irradiated solutions were measured by pH meter (Elico, LI 617). Pyrex borosilicate glass tubes of 2.5 cm diameter and 8 cm length containing aqueous dye solution of 30 ml was subjected to irradiation studies.

### 2.2. Radiolysis of aqueous dye solution by gamma radiation

Irradiation of aqueous dye solutions were carried out at the dose rate of  $2.5 \text{ kGy}\cdot\text{h}^{-1}$  (Fricke dosimeter) using  $^{60}\text{Co}$  source gamma chamber (Meat Technology Unit, Kerala Veterinary and Animal Sciences University, Kerala, India). UV-Visible spectrometer (Eppendorf – Kinetic, Germany) was used to monitor the absorption spectra and changes in concentration of dye during degradation. The percentage of degradation was determined using Eq. (2)

$$\text{Degradation (\%)} = \left[ \frac{A_b - A_f}{A_b} \right] * 100 \quad (2)$$

where  $A_b$  and  $A_f$  are the maximum absorbance of the dye solution before and after irradiation respectively.

## 3. Computational & mathematical modelling using artificial neural network (ANN)

The best possible results could be obtained for a process by using computational models with limited experiments [13]. The influence of the process parameters and the kinetic parameters of the various intermittent steps involved in the reaction are very difficult to determine due to the complexity in understanding the mechanism of augmented radiolysis using hydrogen peroxide. This is caused by the complexity in solving the stoichiometric expressions and

Table 1  
Characteristics of Reactive dyes

Parameters	Reactive Orange 16	Reactive Red 120	Direct Red 80
Colour Index Number	17757	292775	35780
Molecular formula	$C_{20}H_{17}N_3Na_2O_{11}S_3$	$C_{44}H_{24}C_{12}N_{14}O_2S_6Na_6$	$C_{45}H_{26}N_{10}Na_6O_{21}S_6$
Molecular Mass (g/mol)	617.54	1469.98	1373.07
$\lambda_{max}$ (nm)	494	536	528
Chemical class	Monoazo	Diazo	Polyazo
Chemical Structure			

the equations of the radiant energy balance, the spatial distribution of the absorbed radiation and the rate of recombination of free radical species. Thus artificial neural network architecture was chosen to simulate and model the process of degradation of reactive dyes as it does not require the mathematical description of the intermittent steps involved in the process. All ANN calculations were carried out using Matlab 7.0 mathematical software. The architecture of ANN is the statistical outcome based on the inspiration from the human brain network, where billions of neurons are interconnected towards signal transmission. In general, parallel interconnected multi layered perceptron consists of: (1) independent variables – input layer, (2) number of hidden layers, (3) dependent variables - output layer. The number of input and output neurons is fixed by the nature of the problem and a network with single hidden layer with large number of neurons can interpret any input-output structure [14]. Number of layers in the network [15], the number of nodes in each layer and the nature of the transfer functions determines the topology of an ANN [16].

In this study, three artificial neural network (ANN) models were developed for the prediction and simulation of the degradation of reactive dyes (Reactive Orange 16 - Monoazo; Reactive Red 120 - Diazo; Direct Red 80 - Poly azo) in aqueous solution by high energy gamma radiation. The input and output variables were selected based on previous work [6] and it is listed in the Table 2. A three-layer feed-forward network was trained using 750 sets of input–output response with sigmoid hidden neurons and linear output neurons developed with Levenberg–Marquardt back propagation algorithm (trainlm) was used to develop three different networks. 70% of these input-output response was used to train the network, 15% were used for validation and 15% were used for testing the model. The input variables to the feed forward network were as follows: Concentration of  $H_2O_2$  (mM), Dose of gamma ray (kGy), pH, Concentration of dye (mg/L). The percentage of degradation was chosen as the experimental response or output variable.

## 4. Results & discussion

### 4.1. Optimization of neurons number

The minimum value of mean squared error (MSE) of the training was used to predict the optimum number of neurons [17]. The lower the MSE, the higher the accuracy of prediction as there would be excellent match between the

Table 2  
Model variables and their ranges

Variable	Range
Input layer	
Concentration of $H_2O_2$ (mM)	0–2.0
Dose of gamma ray (kGy)	1–6
pH	3.0–11.0
Concentration of dye (mg/L)	100–500
Output layer	
Degradation (%)	0–100

actual and predicted data set. Levenberg–Marquardt back propagation algorithm was used to optimize the neurons in the range of 2–14. Each topology was repeated twice to avoid random initialization of weights leads to random correlation. The mean square error was used as the error function. MSE measures the network performance according to the following Eq. (3):

$$MSE = \frac{1}{Q} \sum_{i=1}^{i=Q} (y_{i,pred} - y_{i,exp})^2 \quad (3)$$

where  $Q$  is the number of data point, prediction through network, experimental response and  $i$  is an index of data. Fig. 1 shows the relationship between the MSE and number of neurons. MSE value was found to decrease as the number of neurons increased up to 10, beyond which MSE value increased. Hence, 10 neurons were selected as the best number of neurons. Optimized neural network structure is shown in Fig. 2.

### 4.2. Test and validation of the model

The efficiency of the models was tested and validated in two different aspects using (i) (30% = 15 + 15) of the input–output data in the studied range; (ii) sets of input operated at pH 6.0 and 12.0. Figs. 3a, 3b, 3c show the comparison

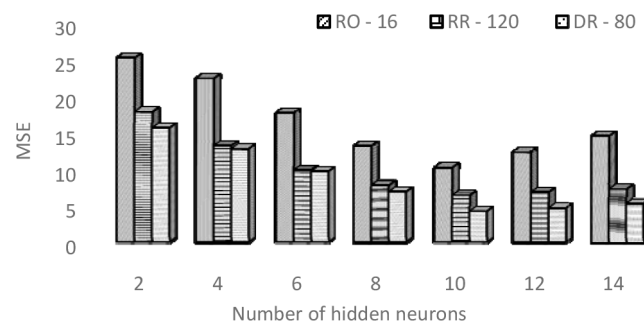


Fig. 1. Effect of the number of neurons in the hidden layer on the performance of the neural network.

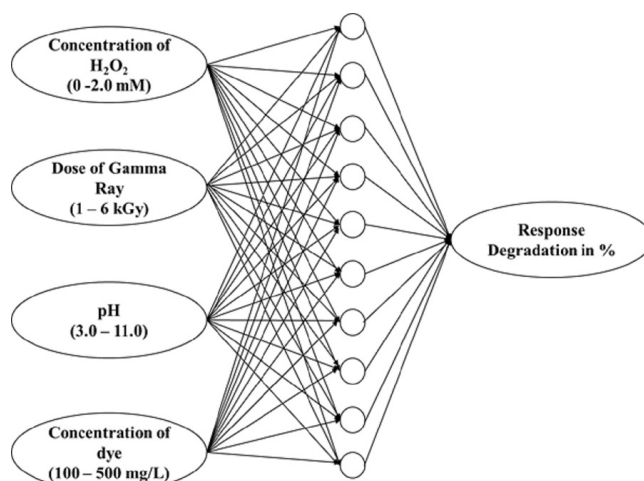


Fig. 2. The optimized artificial neural network architecture.

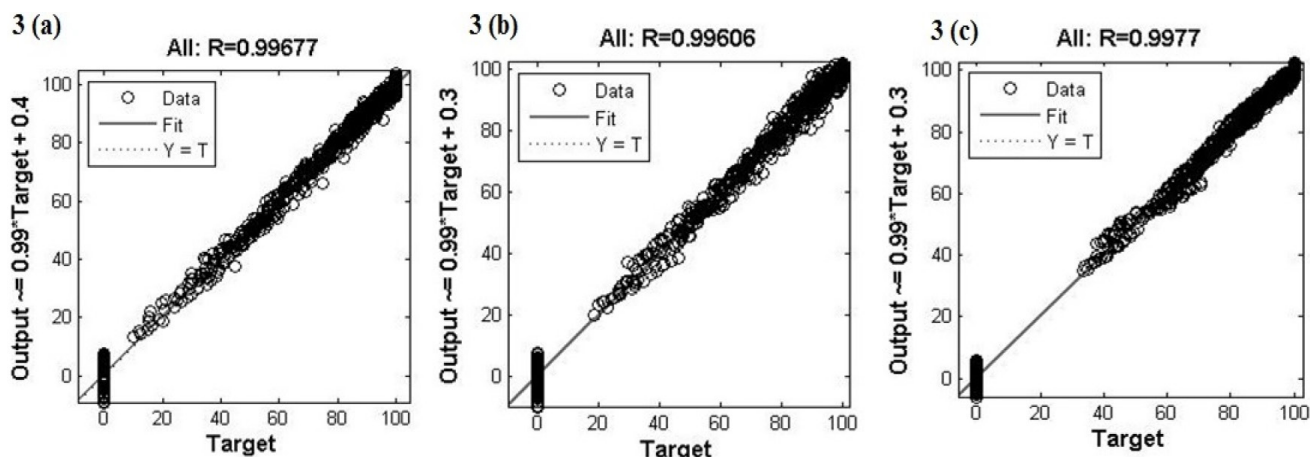


Fig. 3. Comparison between the actual (target) and predicted (output) values for the degradation of (a) RO16; (b) RR120; (c) DR80 in the studied range.

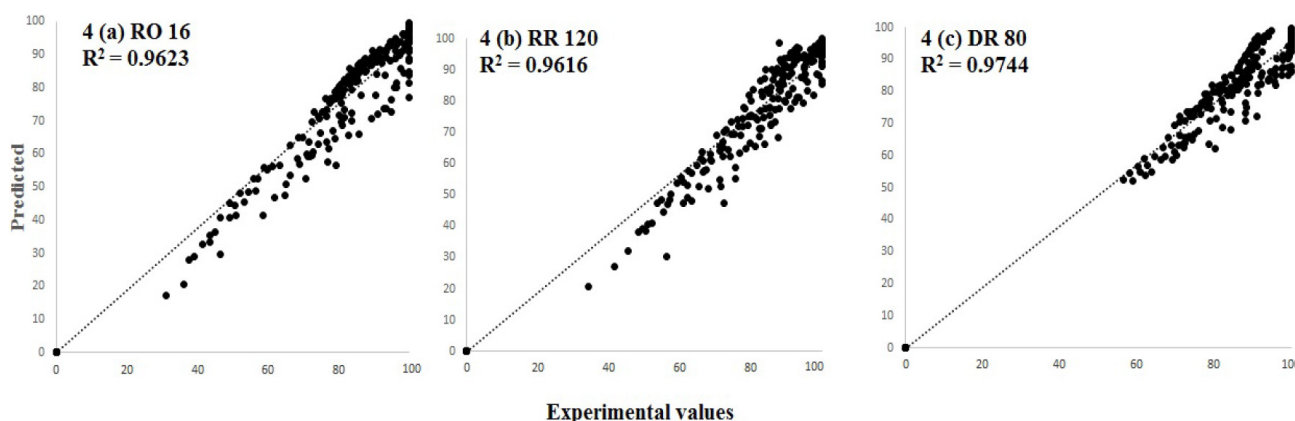


Fig. 4. Comparison between the actual (target) and predicted (output) values for the degradation of (a) RO16; (b) RR120; (c) DR80 operated at pH 6.0 & 12.0.

between the actual experimental values and predicted values using the neural network model for RO16, RR120, and DR80 dyes in the studied range. The overall  $R^2$  for the trained model was found to be 0.99677, 0.99606 and 0.9977 for the degradation of RO16, RR120, and DR80 respectively. Figs. 4a, 4b, 4c show the comparison between the actual experimental values and predicted values using the neural network model for RO16, RR120, and DR80 dyes operated at pH 6.0 & 12.0. The  $R^2$  for the trained model was found to be 0.9623, 0.9616 and 0.9744 for the degradation of RO16, RR120, and DR80 respectively. Based on the MSE value, the number of neurons are optimized to predict the experimental data. The MSE value for the trained networks converges to very low value as the number of epochs increases. The MSE value for the training, validation and testing component of the network corresponding to RO-16 converges to 10.352 by 79 epochs whereas MSE value converges to 6.51 and 4.24 by 38 and 35 epochs for RR-120 and DR-80 respectively. The  $R^2$  value for the trained networks including training, validation and testing are greater than 0.95 indicates the higher linear in the correlation of the variables.

### 4.3. Sensitivity analysis

The relative importance of the input variables were assessed based on the neural net weight matrix and Garson equation [18]. He proposed an equation based on the partitioning of connection weights:

$$I_j = \frac{\sum_{m=1}^{m=Nh} (|W_{jm}^{ih}| / \sum_{k=1}^{Ni} |W_{km}^{ih}|) \times |W_{mn}^{ho}|}{\sum_{k=1}^{k=Ni} \left\{ \sum_{m=1}^{m=Nh} (|W_{jm}^{ih}| / \sum_{k=1}^{Ni} |W_{km}^{ih}|) \times |W_{mn}^{ho}| \right\}} \quad (4)$$

where,  $I_j$  is the relative importance of the  $j^{th}$  input variable on the output variable,  $N_i$  and  $N_h$  are the number of input and hidden neurons, respectively and  $W$  is connection weight, 'i', 'h' and 'o' refers to input, hidden and output layers, respectively and 'k', 'm' and 'n' refers to input, hidden and output neurons respectively. Tables 3, 4, 5 show the weights between the artificial neurons produced by the ANN model used in this work for the degradation of RO16, RR120, and DR80 respectively. Table 6 shows the relative importance of the input variables calculated by

Table 3

Matrix of weights for the degradation of RO16 dye.  $W_1$ : Weights between input and hidden layers;  $W_2$ : weights between hidden and output layers

Neuron	$W_1$				$W_2$			
	Variable				Concentration of dye (mg/L)	Bias	Neuron	Weight
	Conc. of $H_2O_2$ (mM)	Dose of gamma ray (kGy)	pH					
1	-0.03937	-0.21668	0.021644	0.00437	-1.33094	1	-40.2329	
2	-0.31858	0.112985	-1.04724	0.000969	3.384988	2	-4.99483	
3	-14.8443	9.916626	-9.89097	0.057645	-7.76603	3	-1.28509	
4	-1.64179	-0.00857	-0.03211	0.001404	2.353289	4	15.74417	
5	-24.0191	18.34196	-3.79699	-0.20183	29.20936	5	-1.37549	
6	0.256621	0.19346	-0.04941	-0.00453	-1.35895	6	6.562788	
7	11.14552	16.27033	12.75889	-0.23057	5.729084	7	0.230411	
8	-0.00128	0.616722	0.022156	0.00186	-0.50881	8	73.1977	
9	-0.66514	0.023626	0.080593	-0.00045	-0.15614	9	-23.2219	
10	37.71599	1.736083	1.416726	-0.50784	-15.335	10	1.656467	
						Bias	-23.1881	

Table 4

Matrix of weights for the degradation of RR 120 dye.  $W_1$ : Weights between input and hidden layers;  $W_2$ : weights between hidden and output layers

Neuron	$W_1$				$W_2$			
	Variable				Concentration of dye (mg/L)	Bias	Neuron	Weight
	Conc of $H_2O_2$ (mM)	Dose of gamma ray (kGy)	pH					
1	-36.8616	32.61613	57.325	-49.3464	-5.23251	1	-0.03455	
2	-0.05086	-3.97203	-0.00994	-5.61153	2.084585	2	0.510117	
3	0.296892	-1.27529	-8.33279	-0.85976	2.171343	3	0.052518	
4	0.044023	3.427533	0.007733	-0.00528	3.61477	4	2.058187	
5	0.094073	1.089047	0.052892	1.239413	-0.7189	5	0.738986	
6	-2.24739	-13.1314	28.31278	-33.2364	-9.98741	6	0.016637	
7	-23.0164	-7.57906	-11.2316	-17.1673	-2.98278	7	-0.04274	
8	-5.69614	7.352011	-0.17758	-0.16809	0.850365	8	-0.06905	
9	-4.53278	-0.03151	-0.21156	0.233117	2.510137	9	0.130723	
10	-0.06503	8.581021	0.099535	-10.7548	-2.60915	10	0.228356	
						Bias	-1.1538	

Eq. (4). Three variables have strong effect on reactive dye degradation in terms of percentage of degradation. Dose of gamma ray (kGy) appears to be more influencing variable followed by concentration of  $H_2O_2$  (mM) and pH, whereas the concentration of dye (mg/L) has relatively low importance.

#### 4.4. Effect of dose of gamma ray

To examine the effect of dose of gamma ray on the degradation of reactive dyes, the solution containing  $H_2O_2$  (0.5 mM) and 500 mg/L of reactive dye was irradiated with gamma ray of dose 1–6 kGy. The initial pH of the solution

was 5.0. Fig. 5a shows the effect of dose of gamma rays on the degradation of three different reactive dyes. As the dose of gamma ray increases from 1 to 6 kGy, the percentage of degradation also increases from 29.58 to 79.45, 32.03 to 76.16 and 46.69 to 83.57 for RO16, RR120 and DR80 respectively. Radiolysis of water using high energy gamma radiation results in the generation of highly reactive radicals, which are responsible for the degradation of textile dyes (Eq. (1)). The hydrated electrons, hydrogen atoms and  $\cdot OH$  radicals will react with the dye molecules through diffusion controlled processes. The hydrated electrons and hydrogen atoms have a minimum interaction with the reactive dye molecules. The reduction potentials of reactive dyes are much negative than the reduction potentials of these spe-

Table 5

Matrix of weights for the degradation of DR 80 dye.  $W_1$ : Weights between input and hidden layers;  $W_2$ : weights between hidden and output layers

Neuron	$W_1$			$W_2$			
	Variable			Concentration of dye (mg/L)	Bias	Neuron	Weight
Conc of H <sub>2</sub> O <sub>2</sub> (mM)	Dose of gamma ray (kGy)	pH					
1	3.870942	8.919951	0.055325	-0.096	3.266379	1	3.648555
2	0.181436	0.53904	0.04377	0.002048	-1.31601	2	19.6793
3	-0.62302	0.062993	-0.05166	-0.00211	2.180683	3	16.8994
4	0.209728	6.336979	-0.57017	-0.15838	15.21254	4	3.04581
5	-0.96276	1.223123	-1.0994	-0.07509	-2.56613	5	0.378569
6	-1.02763	-0.04453	0.04239	0.00202	-0.8483	6	-15.8397
7	-0.77672	-1.39033	-0.83335	-0.45089	-1.09236	7	-5.33028
8	-0.66875	-13.3311	8.231035	-0.06327	-13.1788	8	-1.14815
9	-0.11919	-6.99292	0.015984	0.001148	6.022504	9	-22.0645
10	1.931686	-1.26414	-0.04963	-0.000048	-0.87763	10	-3.52026
						Bias	11.46682

Table 6

Relative importance of input variables for the degradation of reactive dyes

Input variables	Relative importance %		
	RO 16 - Monoazo	RR120 - Diazo	DR 80 - Polyazo
Conc. of H <sub>2</sub> O <sub>2</sub> (mM)	28.75	20.47	39.49
Dose of gamma ray (kGy)	62.94	34.33	54.31
pH	7.74	17.43	5.24
Concentration of dye (mg/L)	0.57	27.77	0.96
Total	100	100	100

cies (hydrated electrons and hydrogen atoms), these species could not reduce the reactive dyes. Hence, the hydroxyl radicals alone could able to reduce the reactive dyes [19].

#### 4.5. Effect of pH

The generation of hydroxyl radicals is influenced by the pH of the solution [20]. To investigate the effect of initial pH on the degradation of reactive dyes, the experiments were done by varying the pH in the range of 3.0–11.0 where the initial concentration of H<sub>2</sub>O<sub>2</sub>, concentration of dye and dose were kept constant as 0.5 mM, 500 mg/L and 6 kGy respectively. Fig. 5b shows the pattern of degradation in the chosen range of pH. Though there is not much significant difference in the percentage of degradation with respect to different pH and different dyes, the maximum percentage of degradation was observed in the acidic range. The degradation efficiency of the reactive dyes during radiolysis depends on the kind of active species generated based on the pH of the solution. In acidic solution, the decreased interaction between  $e_{aq}^-$  and  $\cdot OH$  leads to the increased concentration of  $\cdot OH$  and the formation of  $\cdot H$  increases the rate of degradation. In alkaline condition,  $\cdot OH$  easily reacts with

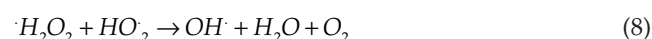
$OH^-$  to form water, thereby the availability of  $\cdot OH$  for the degradation process is limited [21,22].



From the results, the increased percentage of degradation at low pH and the decreased percentage of degradation at high pH solution demonstrate that  $\cdot OH$  is a main parameter in the degradation of reactive dyes during radiolysis.

#### 4.6. Effect of H<sub>2</sub>O<sub>2</sub>:

The effect of H<sub>2</sub>O<sub>2</sub> on the degradation of reactive dyes were examined by varying the concentration of H<sub>2</sub>O<sub>2</sub> from 0.5 to 2 mM at constant dose: 6 kGy, concentration of dye: 500 mg/L and pH: 5.0. The results as shown in Fig. 5c, the degradation of reactive dyes by radiolysis is enhanced by the addition of H<sub>2</sub>O<sub>2</sub>. The increase in percentage of degradation was observed as the concentration of H<sub>2</sub>O<sub>2</sub> was increased to 1 mM and it starts to decrease after 1 mM. The degradation reaction is enhanced due to the increase in the  $\cdot OH$  radicals due to the increase in concentration of H<sub>2</sub>O<sub>2</sub>. The decrease in degradation was observed as the concentration of H<sub>2</sub>O<sub>2</sub> is increased above 1.0 mM because of scavenging of  $\cdot OH$  radicals by excess H<sub>2</sub>O<sub>2</sub> [23,24].



## 5. Conclusion

A three-layer feed-forward network was trained and optimized to predict the degradation of reactive dyes using

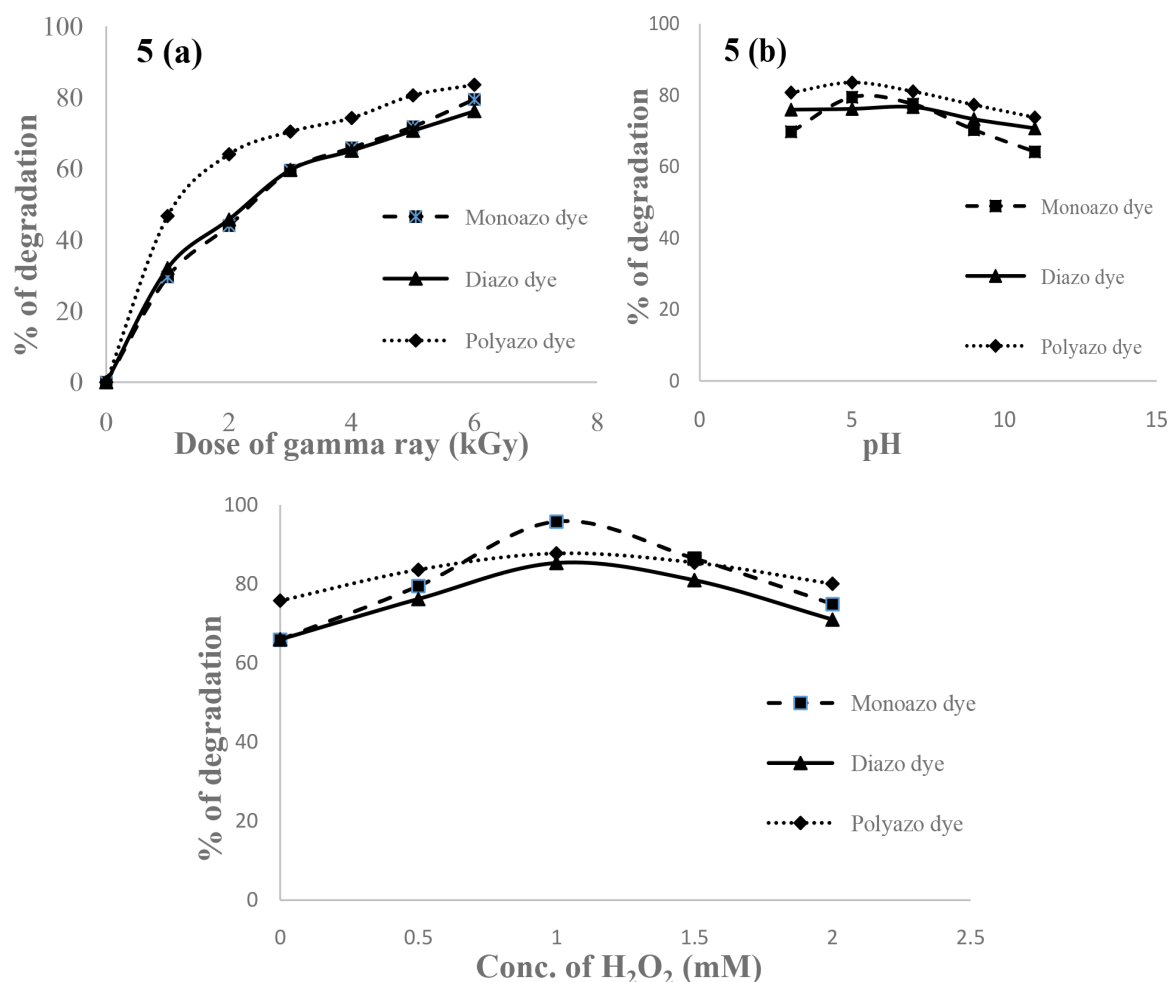


Fig. 5. (a) Effect of dose of gamma ray; (b) Effect of pH; (c) Effect of H<sub>2</sub>O<sub>2</sub> on the degradation of reactive dyes.

high energy gamma radiation. The Levenberg–Marquardt back propagation algorithm was used to optimize the neurons in the range of 2–14 based on the low MSE value and it was optimized as 10 neurons. ANN predicted results are very close to the experimental results in all three networks with  $R^2 > 0.96$  in both different validation methods. The sensitivity analysis showed that three variables have strong effect on removal of reactive dyes in terms of percentage of degradation. Dose of gamma ray (kGy) appears to be more influencing variable followed by concentration of H<sub>2</sub>O<sub>2</sub> (mM) and pH whereas the concentration of dye (mg/L) has relatively low importance. ANN results showed that modelling based on trained neural network could effectively simulate and predict the behavior of the degradation of reactive dyes using high energy gamma radiation.

#### Acknowledgement:

The authors are thankful to Tamilnadu State Council for Science and Technology, India for providing an opportunity to do collaborative research through Young Scientist fellowship. One of the author (V.C. Padmanaban) is thankful to BRNS-BARC, Mumbai for providing research grant to carry

out this research project (BRNS file number: 2013/20/35/10/BRNS/34). The authors are grateful to Dr. P Subathra, Professor, Department of Information technology, Kamaraj College of Engineering and Technology, India for her valuable suggestions in Artificial Neural Network modelling.

#### References

- [1] M.F. Akhtar, M. Ashraf, A.A. Anjum, A. Javeed, A. Sharif, A. Saleem, B. Akhtar, Textile industrial effluent induces mutagenicity and oxidative DNA damage and exploits oxidative stress biomarkers in rats, *Environ. Toxicol. Pharmacol.*, 41 (2016) 180–186.
- [2] L. Abdou, O. Hakeim, M. Mahmoud, A. El-Naggar, Comparative study between the efficiency of electron beam and gamma irradiation for treatment of dye solutions, *Chem. Eng. J.*, 168 (2011) 752–758.
- [3] V.K. Gupta, R. Jain, A. Nayak, S. Agarwal, M. Shrivastava, Removal of the hazardous dye–tartrazine by photo degradation on titanium dioxide surface, *Mater. Sci. Eng. C.*, 31 (2011) 1062–1067.
- [4] V.C. Padmanaban, M.G. Nandagopal, A. Achary, V.N. Vasudevan, N. Selvaraju, Optimisation of radiolysis of Reactive Red 120 dye in aqueous solution using ionizing <sup>60</sup>Co gamma radiation by response surface methodology, *Water Sci. Technol.*, 73 (2016) 3041–3048.

- [5] J. Biswal, J. Paul, D. Naik, S. Sarkar, S. Sabharwal, Radiolytic degradation of 4-nitrophenol in aqueous solutions: Pulse and steady state radiolysis study, *Radiation Phys. Chem.*, 85 (2013) 161–166.
- [6] V. Padmanaban, N. Selvaraju, V. Vasudevan, A. Achary, Augmented radiolytic ( $^{60}\text{Co } \gamma$ ) degradation of direct red 80 (Polyazo dye): optimization, reaction kinetics and G-value interpretation, *React. Kinetics Mech. Catal.*, 1–15.
- [7] M. Wang, R. Yang, W. Wang, Z. Shen, S. Bian, Z. Zhu, Radiation-induced decomposition and decoloration of reactive dyes in the presence of  $\text{H}_2\text{O}_2$ , *Radiation Phys. Chem.*, 75 (2006) 286–291.
- [8] D. Salari, A. Niaei, A. Khataee, M. Zarei, Electrochemical treatment of dye solution containing CI Basic Yellow 2 by the peroxi-coagulation method and modeling of experimental results by artificial neural networks, *J. Electroanal. Chem.*, 629 (2009) 117–125.
- [9] M.A. Behnajady, H. Eskandarloo, F. Eskandarloo, Artificial neural network modeling of the influence of sol-gel synthesis variables on the photo catalytic activity of  $\text{TiO}_2$  nanoparticles in the removal of Acid Red 27, *Res. Chem. Intermed.*, 41 (2015) 6463–6476.
- [10] M. Pirdashti, S. Curteanu, M.H. Kamangar, M.H. Hassim, M.A. Khatami, Artificial neural networks: applications in chemical engineering, *Rev. Chem. Eng.*, 29 (2013) 205–239.
- [11] G. Lenzi, R. Evangelista, E. Duarte, L. Colpini, A. Fornari, R. Menechini Neto, L. Jorge, O. Santos, Photo catalytic degradation of textile reactive dye using artificial neural network modeling approach, *Desal. Water Treat.*, 57 (2016) 14132–14144.
- [12] M. Tanzifi, M.T. Yarak, A.D. Kiadehi, S.H. Hosseini, M. Olazar, A.K. Bhati, S. Agarwal, V.K. Gupta, A. Kazemi, Adsorption of Amido Black 10B from aqueous solution using polyaniline/ $\text{SiO}_2$  nano composite: Experimental investigation and artificial neural network modeling, *J. Colloid Interface Sci.*, 510 (2018) 246–261.
- [13] E. Maleki, N. Maleki, Artificial neural network modeling of Pt/C cathode degradation in PEM fuel cells, *J. Electron. Mater.*, 45 (2016) 3822–3834.
- [14] D. Salari, N. Daneshvar, F. Aghazadeh, A. Khataee, Application of artificial neural networks for modeling of the treatment of wastewater contaminated with methyl tert-butyl ether (MTBE) by UV/ $\text{H}_2\text{O}_2$  process, *J. Hazard. Mater.*, 125 (2005) 205–210.
- [15] N. Daneshvar, A. Khataee, N. Djafarzadeh, The use of artificial neural networks (ANN) for modeling of decolorization of textile dye solution containing CI Basic Yellow 28 by electro coagulation process, *J. Hazard. Mater.*, 137 (2006) 1788–1795.
- [16] D.N. Kartic, B.C.A. Narayana, M. Arivazhagan, Removal of high concentration of sulfate from pigment industry effluent by chemical precipitation using barium chloride: RSM and ANN modeling approach, *J. Environ. Manage.*, 206 (2018) 69–76.
- [17] K. Yetilmeszooy, S. Demirel, Artificial neural network (ANN) approach for modeling of Pb (II) adsorption from aqueous solution by Antep pistachio (*Pistacia Vera L.*) shells, *J. Hazard. Mater.*, 153 (2008) 1288–1300.
- [18] G.D. Garson, Interpreting neural-network connection weights, *AI expert.*, 6 (1991) 46–51.
- [19] C.C. Guaratini, A.G. Fogg, M.V.B. Zanoni, Assessment of the application of cathodic stripping voltammetry to the analysis of diazo reactive dyes and their hydrolysis products, *Dyes Pigments*, 50 (2001) 211–221.
- [20] E.S. Elmolla, M. Chaudhuri, M.M. Eltoukhy, The use of artificial neural network (ANN) for modeling of COD removal from antibiotic aqueous solution by the Fenton process, *J. Hazard. Mater.*, 179 (2010) 127–134.
- [21] A.A. Basfar, H.M. Khan, A.A. Al-Shahrani, Trihalomethane treatment using gamma irradiation: kinetic modeling of single solute and mixtures, *Radiation Phys. Chem.*, 72 (2005) 555–563.
- [22] Z. Guo, Q. Dong, D. He, C. Zhang, Gamma radiation for treatment of bisphenol A solution in presence of different additives, *Chem. Eng. J.*, 183 (2012) 10–14.
- [23] N. Suzuki, T. Nagai, H. Hotta, M. Washino, The radiation-induced degradation of azo dyes in aqueous solutions, *Int. J. Appl. Radiation Isotopes*, 26 (1975) 726–730.
- [24] A. Swallow, In: J.H. Baxendale, F. Busi, The study of fast processes and transient species by electron pulse radiolysis, Springer 1982, pp. 289–315.